UNIVERSITAT JAUME I

Degree final project

Functionalization of glass fibers from plastic waste

Author

Alejandro Ruiz Gomis

Tutor

Juan Bautista Carda Castelló

Chemical Degree

2017/2018

Abstract

Mullite has achieved outstanding importance as a material for both traditional and advanced ceramics because of its favourable thermal and mechanical properties. Mullite displays various Al to Si ratios referring to the solid solution $Al_{4+2x}Si_{2-2x}O_{10-x}$, with x ranging between about 0.2 and 0.9 (about 55 to 90 mol% Al_2O_3) [1]. In this work, the functionalization of the recycled glass fibers (obtained from the glycolysis process) with mullite crystals and its introduction into the precursor composition of the ceramic substrate was proposed. Mullite were first prepared by sol-gel method using colloidal silica and $AlCl_3 \cdot 6H_2O$ in water system. The gel mullite precursor was fired in the range 1000-1300ºC soaking times 30–300 min. The resultant materials were studied by X-Ray diffraction (XRD) and scanning electron microscope (SEM-EDX). On the other hand, the glass fibers were functionalizing through the previous mullite synthesized. Several porcelain stoneware tile compositions were prepared using high alumina clay, low alumina clay, kaolin, Turkish feldspar (Na), feldspar (Na/Mg), feldespathic sand and glass fiber functionalize. The resultant materials were studied by X-Ray diffraction (XRD), scanning electron microscope (SEM-EDX) and compressive test. High mechanical resistance ceramic material (> 450 Kg/cm^2) was obtained.

Index

1. Introduction

1.1 Mullite

Mullite is a mineral that belongs to the family of nesosilicates, which are very rare in nature. The most important deposit is on the island of Mull, in the western part of Scotland, where it has been formed under conditions of pressure and temperature very similar to those that are necessary to obtain it artificially. In addition to the elements of its composition, usually carry as impurities: titanium, iron, sodium and potassium [1]. Mullite is used in the manufacture of ceramics, which crystallizes in the orthorhombic system in crystals that are elongated and improve the properties of ceramics[2]. One of the most common crystalline phases in ceramics having nominal composition $3Al_2O_3 \cdot 2SiO_2$ (72 wt% Al_2O_3 and 28 wt% SiO_2) [3-5].

The importance of the use of mullite in ceramics has great importance in recent years. It can be explained by:

- It is the only stable crystalline phase, at normal pressure, in the binary $Al_2O_3 \cdot SiO_2$ system. This material shows excellent properties: high-temperature strength, creep resistance, low thermal expansion coefficient, good chemical and thermal stability, with retention of mechanical properties to elevated temperature and stability in oxidative atmospheres. [5-7].

- The fact that the starting materials are available in big quantities on earth. Thereby kaolinite and other clay-based materials achieved high importance.

- Its ability to form mixed crystals in a wide Al_2O_3/SiO_2 range and to incorporate a large variety of foreign cations into the structure.

There are three types of polycrystalline ceramic mullite that can be differenciated:

Monolithic mullite ceramics

Monolithic mullite ceramics have widely been used for both traditional and advanced applications. Important materials such as porcelain, construction and engineering ceramics and other advanced ceramics such as an optically translucent ceramic for high temperature oven windows[8-9]

Mullite coatings

Many metals and ceramics are susceptible to degradation when exposed to oxidizing, reducing or to other harsh chemical environments at high temperature. A suitable way to overcome these problems is to protect such materials by surface coatings with compounds being stable under the required conditions[10-12].

Mullite matrix composites

This group of materials includes composite materials with mullite matrices and mullite fibers. The main aim is the reduction of the inherent brittleness of the systems by improvement of their toughness. Important application fields of such composites are components and structures for gas turbine engines, high performance furniture, etc. [13-14].

1.1.1 Crystal chemistry of mullite

The formula of mullite is expressed as $Al_{4+2x}Si_{2-2x}O_{10-x}$, with *x* ranging between about 0.2 and 0.9. There are different types of mullite depending on their synthesis:

- Sinter-mullite: Produced by thermal treatment of the starting materials via solid-state reactions. The phase that is obtained is the mullite 3/2 and x =0.25 ($3Al_2O_3{\cdot}2SiO_2$)[15-16].

- Fused-mullite: Produced by crystallizing of alumino silicate melt. They are usually rich in Al_2O_3 with a composition of 2/1 and x = 0.40 ($2Al_2O_3{\cdot}SiO_2$)[17].

- Chemical-mullites: Produced by thermal treatments of precursors of high purity. The composition depends on the starting reagents and the treatment temperature. Extremely rich compounds have been identified in Al_2O_3 (>90 wt.%Al_2O_3, x > 0.80) at synthesis temperatures <1000◦C.

As we have said before, mullite structure derived from sillimanite where the formula is Al_2SiO_5 with x = 0.00. The sillimanite has octahedral chains AlO_6 connected to the edge run parallel to the crystallographic c axis.[18]. In sillimanite, these octahedral chains are crosslinked by double chains with alternating tetrahedra of AlO_4 and SiO_4 (Figure 1).

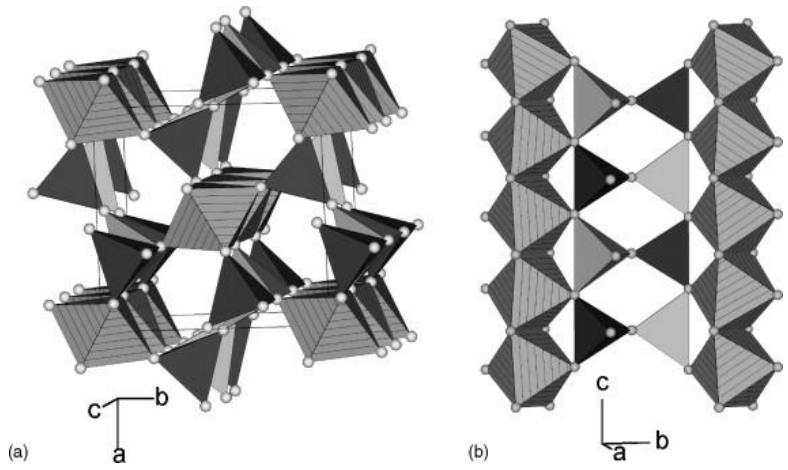

Figure 1. Crystal structure of sillimanite in projections down (a) the *c*-axis, and (b) the *a*-axis.[19]

Mullite is derived from sillimanite by a substitution of Si cations in the tetrahedral holes:

$2Si^{4+} + O^{2-} \rightarrow 2Al^{3+} + \square$ $\square$ = oxygen vacancy.

In this reaction, oxygen atoms are removed from the structure leading to oxygen vacancies. And to a rearrangement and disordering of tetrahedral cations.

Structure refinements indicate that the oxygen atoms bridging two polyhedra in the tetrahedral double chain in sillimanite are removed in mullite. (figure 2).

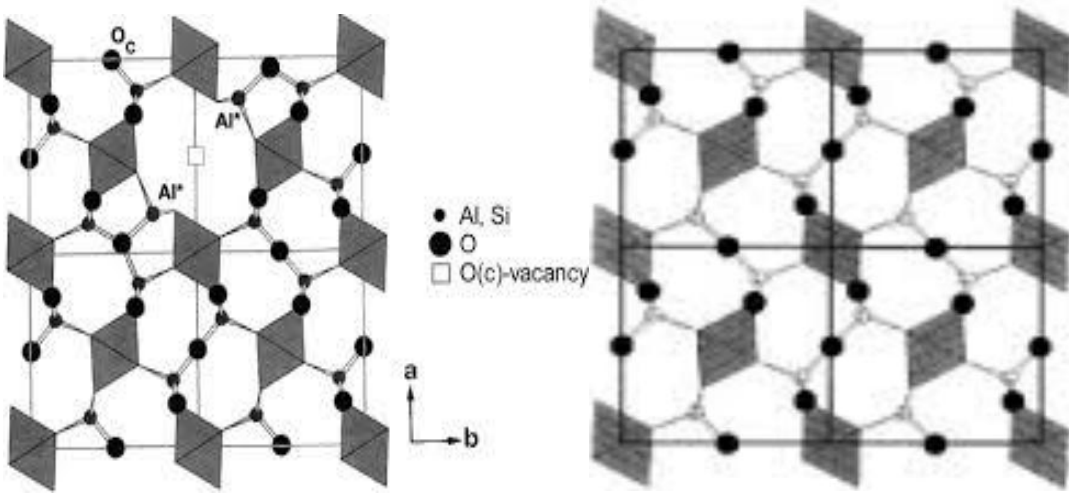

Figure 2. Crystal structure of mullite[20] and sillimanite

On the other hand, figure 3 shows the crystallization of mullite from powder X-ray diffraction patterns [21].

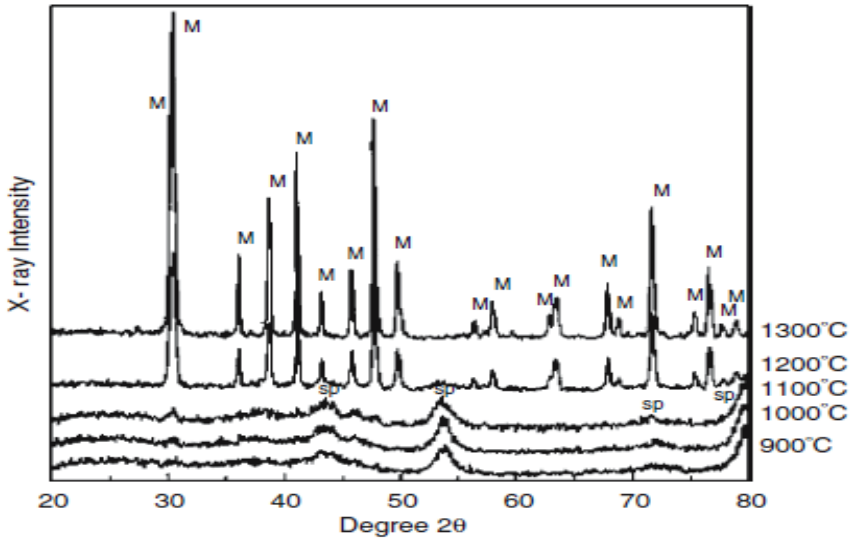

Figure 3. X-ray powder diffraction patterns showing the crystallization of mullite from amorphous precursors as a function of temperature[21]

1.1.2. Al_2O_3-SiO_2 system

Mullite-based ceramics have been used as refractories. In 1924, Bowen and Grieg[22] were the first to publish a phase diagram to include mullite as a stable phase. The mullite phase ($3Al_2O_3 \cdot 2SiO_2$) was reported to melt incongruently at 1810°C.

In 1954, Shears and Archibald [23] reported the presence of a range of solid solution of $3Al_2O_3 \cdot 2SiO_2$ (3:2 mullite) to $2Al_2O_3 \cdot SiO_2$ (2:1 mullite). In 1958, Toropov and Galakhov[24] modified the phase diagram by melting the mullite by heating in a vacuum where the mullite melted congruently at 1850°C .In 1962 Aramaki and Roy[25] prepared their samples from gels for subsolidus thermal treatments.

Aksay and Pask [26] presented the incongruous melting of mullite at 1828°C. Davis and Pask [27] observed coherent mullite growth of sapphire in a temperature range between 1600 and 1800°C, indicating the interdiffusion of aluminum and silicon ions through mullite [26].

Risbud and Pask [28] modified the diagram to incorporate metastable phases regions. At 1890°C of temperature, an incongruent "metastable" melting point was determined. To explain the possibility of metastability, they suggested that there could be a barrier for alumina precipitation both in melt and mullite, and that mullite could be superheated. Figure 4 shows this phase diagram showing the regions of metastability [29].

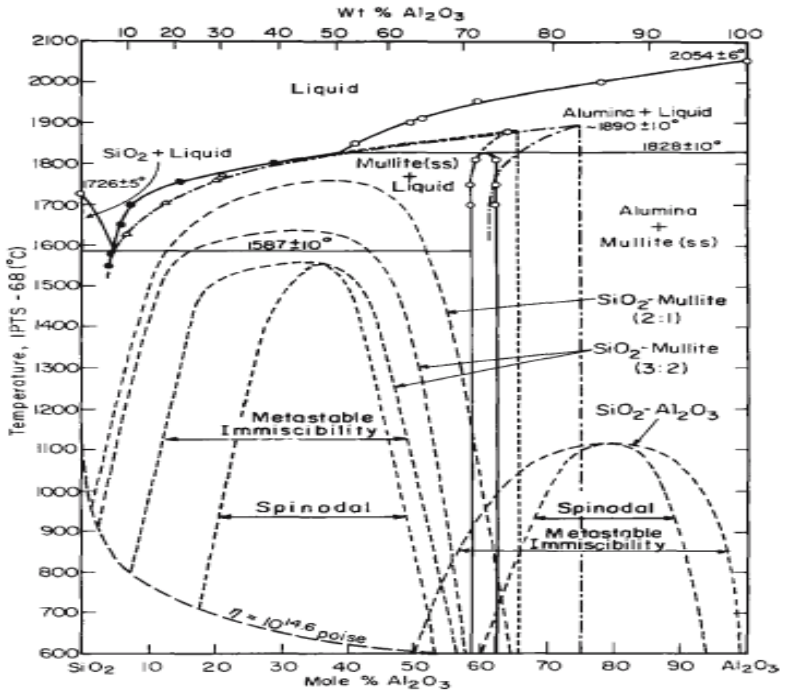

Figure 4. The system Al2O3−SiO2 showing metastable regions. The gaps shown with spinodal regions are considered the most probable thermodynamically[29]

In 1987, Klug et al. [30] observed an incongruent melting of mullite at 1890°C. This phase diagram is in the figure 5 [30]. Mullite 2: 1 seems to be only metastable at room temperature[30], and use at very high temperatures or the use of cycles can cause alumina precipitation. Finally, Pask [31] proposed that the differences on mullite could be due to the content or not of α-Al_2O_3 in the starting materials. Depending on the temperature and pressure, the compound will be sillimanite, kyanite or andalusite.

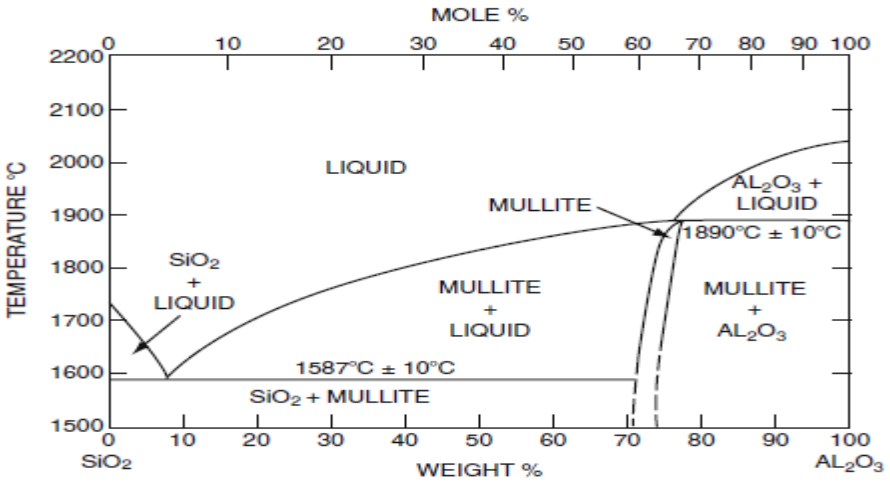

Figure 5. Phase diagram for the alumina–silica system[30]

1.2 Circular economy: Industrial wastes in the ceramic industry

The "Circular Economy" is related to sustainability and aims to ensure that the value of products, materials and resources (water, energy, etc.) is maintained in the economy as long as possible, together with the minimization of waste. The key concept is that it changes from linear to circular economy (see Figure 6)[32]. The circular economy proposes to model of society that optimizes the use of materials, energy and waste[33-35].

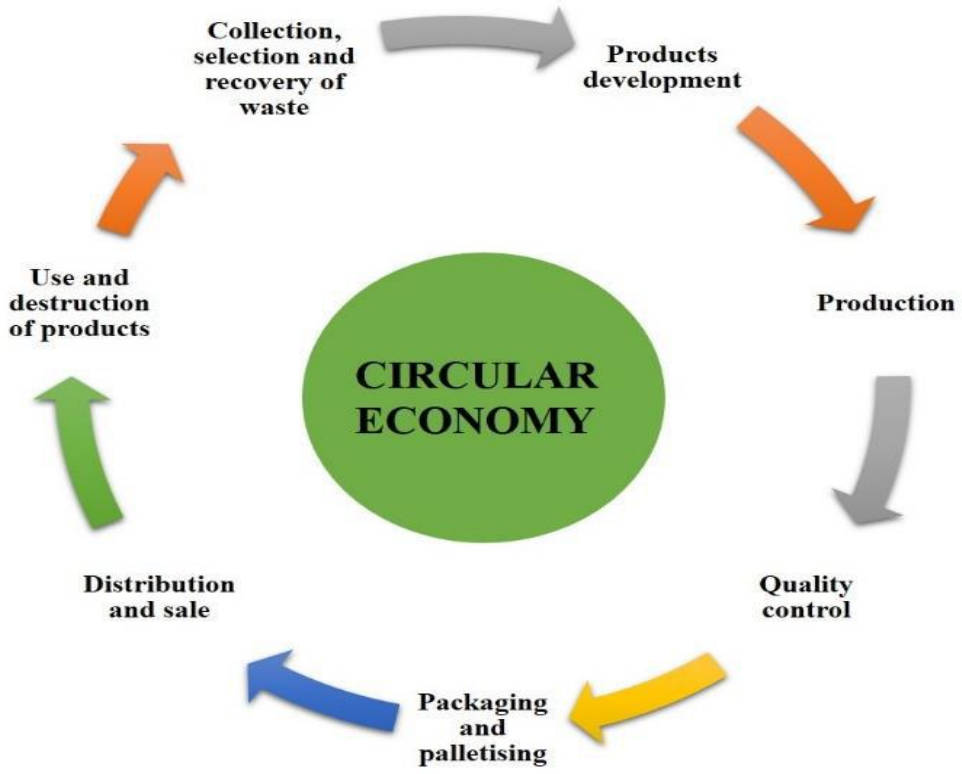

Figure 6. Schematic representation of the circular economy.[32]

1.2.1 Recycling glass fibers

Current recycling technologies for fiberglass composites are divided into mechanical, thermal and chemical methods.

Mechanical recycling

Mechanical recycling consists of minimizing the size of different composite waste in different recycling sizes through grinding processes [36]. The most commonly used technique in mechanical recycling is the hammer mill process.[37-38].

Thermal processes

-Pyrolysis is the most analyzed thermal process. It is carried out with or without oxygen and has recently been carried out in the presence of steam [39]. The matrix deterioration causes an oil, gases and solid products such as fibers, fillers and char[40].

-The fluidized bed process consist in a layer of silica sand is used, for example, fluidized by hot air, whereby the conditions are oxidants. The presence of oxygen is necessary to reduce the formation of carbon, which must be removed [41].

-The microwave-assisted pyrolysis has as main characteristic that it is heated in its core, therefore, the thermal transfer is faster and saves energy. Lester [42] was the first to study this heating method to recycle materials.

Chemical recycling

Chemical recycling immerses glass fiber composite waste in a solvent suitable as water, acid and alcohol at a particular pressure and temperature to liberate the fibers. Kinstle [43] employed a hydrolysis between 220 and 275 ° C.

2. Objetives

In this work, we propose the functionalization of the recycled glass fibers (obtained from the glycolysis process) with mullite crystals and its introduction into the precursor composition of the ceramic substrate to obtain high resistance material.

From this general objective, the most detailed specific objectives are presented below:

-Synthesis of the mullite crystals via sol-gel method.

-Functionalize the glass fibers with the mullite crystals obtained.

-Formulation and preparation a stoneware porcelain tile with the functionalization glass fibers in its composition in order to improve the mechanical properties of ceramic materials and therefore reduce the economic cost.

3. Experimental

3.1. Mullite sol-gel synthesis

Mullite were prepared by sol-gel method using colloidal silica ((purity: 99.9%; Mw: 60.08 g / mol) and $AlCl_3 \cdot 6H_2O$ (purity: 99.5%; Mw: 241.43 / mol)) in water system. The silica was obtained from an industrial company, therefore, not having the data of

the silica, an X-ray fluorescence spectrometry was performed to obtain the purity (Table1).

Table 1. Chemical analysis (FRX) of colloidal silica

SiO_2	SiO_2 (wt%)	CaO (wt%)	TiO_2 (wt%)
SC118406-1	99.9	0.08	0.02

Precursor solution was obtained by dissolving 23.5 mmol of colloidal silica and 42 mmol of aluminium in 50 mL of distilled water. The mullite precursor slurry gradually gelled in a beaker due to the condensation of the SiO_2 catalyzed by $NH_3 \cdot H_2O$ (Figure 7). The wet gel block was naturally dried at 100ºC to evaporate all liquid.

The reaction of mullite formation from during the sintering of the precursors is:

$$2\ SiO_2 + 6\ AlCl_3 \cdot 6\ H_2O \text{ ----------> } 3\ Al_2O_3 \cdot 2\ SiO_2$$

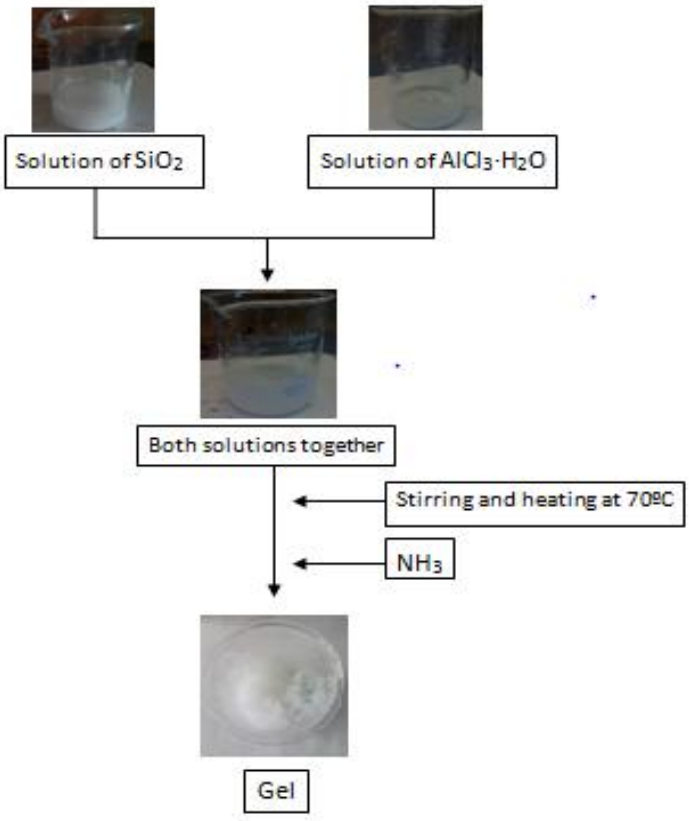

Figure 7. Diagram of the sol-gel synthesis.

Then a crystallization treatment is carried out in a furnace (Nabertherm).

The gel mullite precursor was fired in the range 1000-1300°C soaking times 30-300 minutes with a heat rate of 20°C/min.

Table 2. Thermal treatment conditions

Heating Temperature	Time
1000 °C	30 minutes
1100 °C	30 minutes
1200 °C	30 minutes
1300 °C	30 minutes
1300 °C	1 hour
1300 °C	2 hours
1300 °C	3 hours
1300 °C	4 hours
1300 °C	5 hours

3.2 Functionalization of glass fibers

Previosly, the glass fibers has been grinding using an Agata mortar and a ring mill (Figure 8) to study the influence of fiber size.

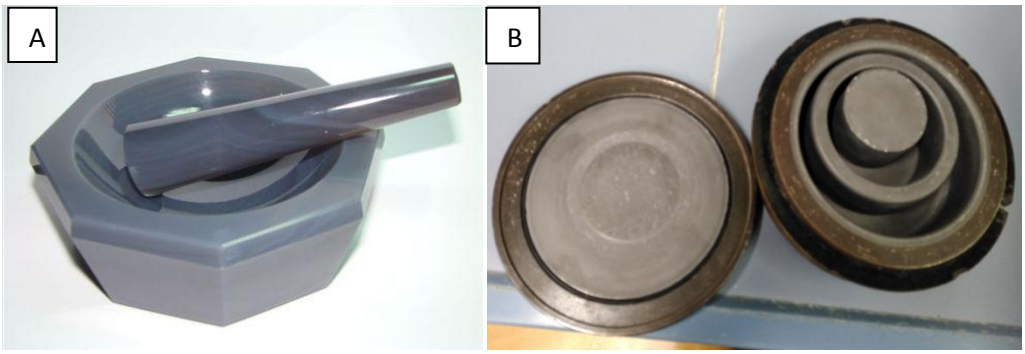

Figure 8. A) Agata mortar. B) Ring mill

A certain amount of glass fibers were suspended in colloidal silica and aluminium solution. After a process of stirring for 30 min and ammonia solution addition, a white gel was formed (Figure 9). The resulting wet gel was drying in oven to

evaporate the solvent. Then the prepared composite was treated at 1300°C during 2 h in order to form mullite crystals. Finally, functionalized glass fibers were to prepare a porcelain stoneware tile composition.

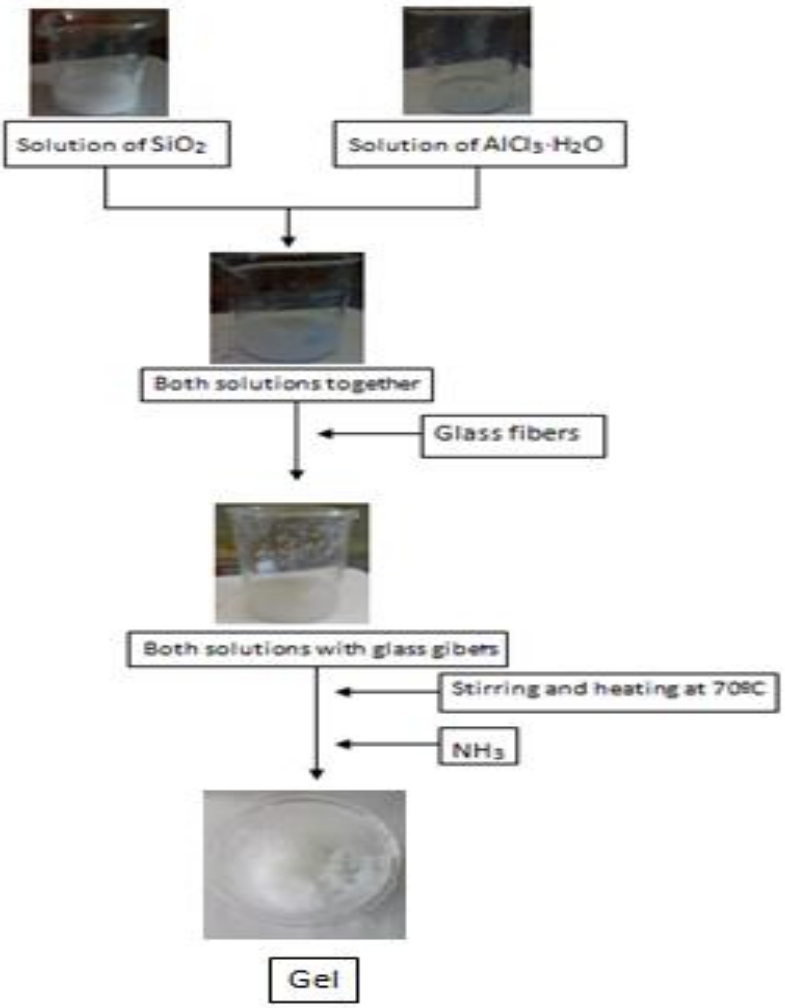

Figure 9. Diagram of the sol-gel synthesis with fiberglass.

The porcelain stoneware tile compositions were prepared using high alumina clay, low alumina clay, kaolin, Turkish feldspar (Na), feldspar (Na/Mg), feldespathic sand and glass fiber functionalize. Each composition was micronized in a planetary alumina ball mill with water and 0.7 wt% of sodium silicate as deffloculant, obtaining a suspension density of 1.70 g/cm^3 and sieved at under 100 µm after been dried. The compositions has been mixed using the mixer of the figure 10 A.

To simulate industrial pressing conditions, the compositions were homogenised and moistened with water to 6.5 wt% to be pressed in a uniaxial laboratory press (Nannetti) similar to figure 10 B, resulting in rectangular pieces with 2.16 g/cm^3 of dried apparent density. After having been dried at 110 °C for 24 h, the pieces were fired at different temperatures in a fast kiln (Nannetti), following the firing cycle shown in figure 11.

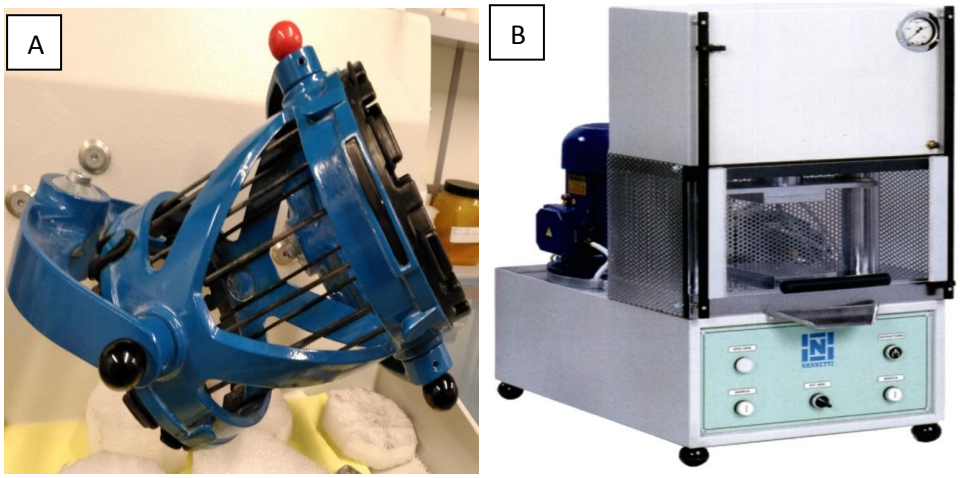

Figure 10. A) Mixer used to obtain homogeneous ceramic composition. B) Hydraulic press.

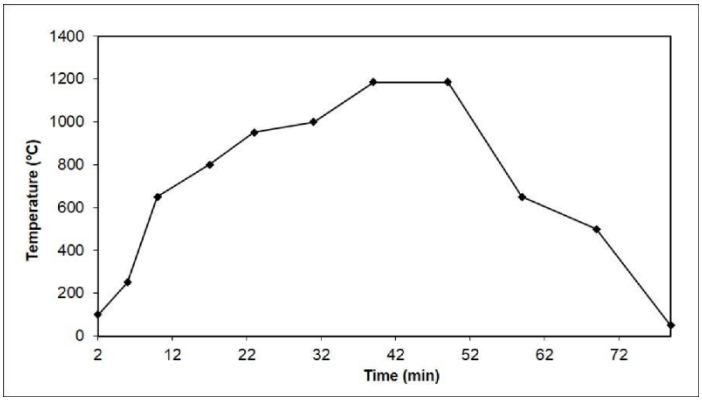

Figure 11. Graph representing the industrial firing cycle used to obtain ceramic porcelain tiles

3.3. Characterization techniques

Colloidal silica composition has been studied by X-Ray Fluorescence (XRF), using a sequential spectrometer X-ray scattering wavelengths S4 Pioneer by Bruker with a Rh X-ray tube of 4 kW. The crystal structure of the materials was characterized by X-ray diffraction (XRD) using a D4 Endeavor, Bruker-AXS equipped with a Cu Kα radiation source. Data was collected by step-scanning from 10º to 80º with step size of 0.05º 2θ

and 1 s counting time per step. Scanning Electron. Microscopy (SEM) model JEOL 7001F attached with an energy dispersive X-ray analysis (EDX) was employed to study the morphology and elemental composition of the samples. The flexural strength, evaluated by a HOYTOM plasticinometer with a load cell of 5000 N and a force threshold of 16N. The size of the particles was analyzed by Coulter counter(LS 230).

4. RESULTS

4.1. Mullite sol-gel synthesis

The X-ray diffraction patterns of the samples after heating at temperatures of 1000 to 1300°C are observed in Figure 12. The phase com positions of all samples were nearly similar, with a phase of mullite ($3Al_2O_3 \cdot 2SiO_2$; JCPDS- 15-0776), α-Al_2O_3 (JCPDS-46-1212) and SiO_2 (JCPDS- 27-0605).

In the case of patterns of the products after heat-treatment at 1000-1100ºC, no diffraction peaks were derived from crystalline phases but broad hallow characteristic of amorphous appeared. Most studies have suggested that the synthesis of the mullite by sol-gel method occurs at 1200-1300°C [44-45]. Above 1300°C, XRD patterns indicated that the products consisted of a mullite phase but with a very intense peak corresponding to corundum.

Figure 13 shows XRD patterns of the products after heat-treatment at 1300°C soaking times 30-300 minutes. The phase com positions of all samples were nearly similar, only increase the cristobalite peak (24º 2 θ). The mullite phase in not the majority, but it is quite repeated. So, the best treatment is for 2 hours because the corundum phase does not appear with great intensity according to the literature[45].

From these conditions, the different tests have been carried out to obtain the porcelain stoneware tiles. It was expected that it could be formed at a lower temperature since the porcelain stoneware is formed at a maximum temperature of 1200°C. For this reason, we have chosen to perform the same procedure in two ways: One has been to perform the procedure with the heat treatment and glass fibers and then introduce it into the ceramic mixture. The other procedure consisted in not

performing the heat treatment that the glass fibers contain and adding it to the ceramic mixture, although with this procedure the mullite phase is not formed.

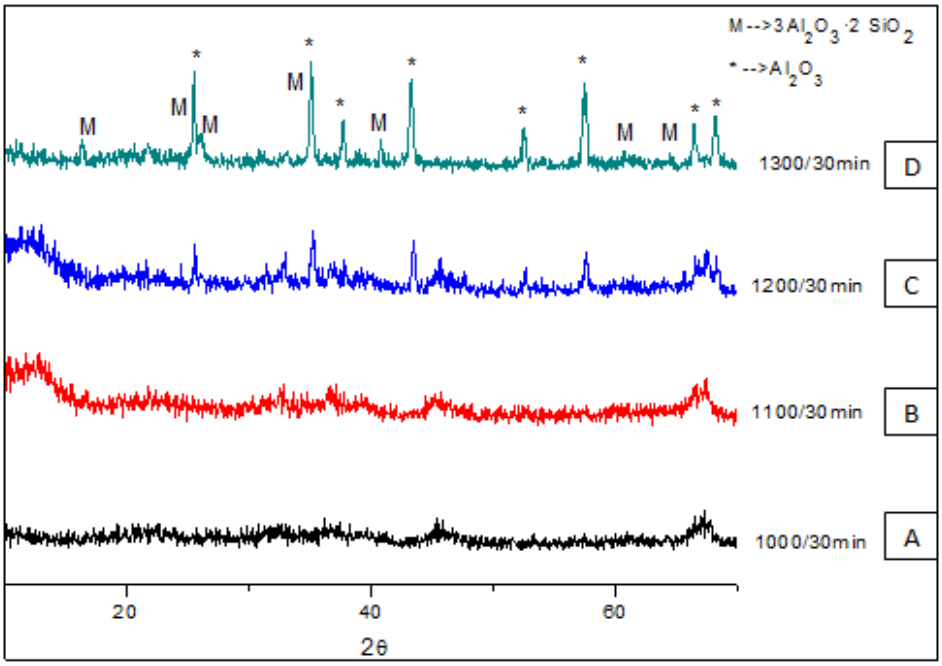

Figure 12. XRD patterns of the products after heat-treatment at (a)1000 ˚C, (b)1100 ˚C, (c)1200 ˚C and (d)1300 ˚C

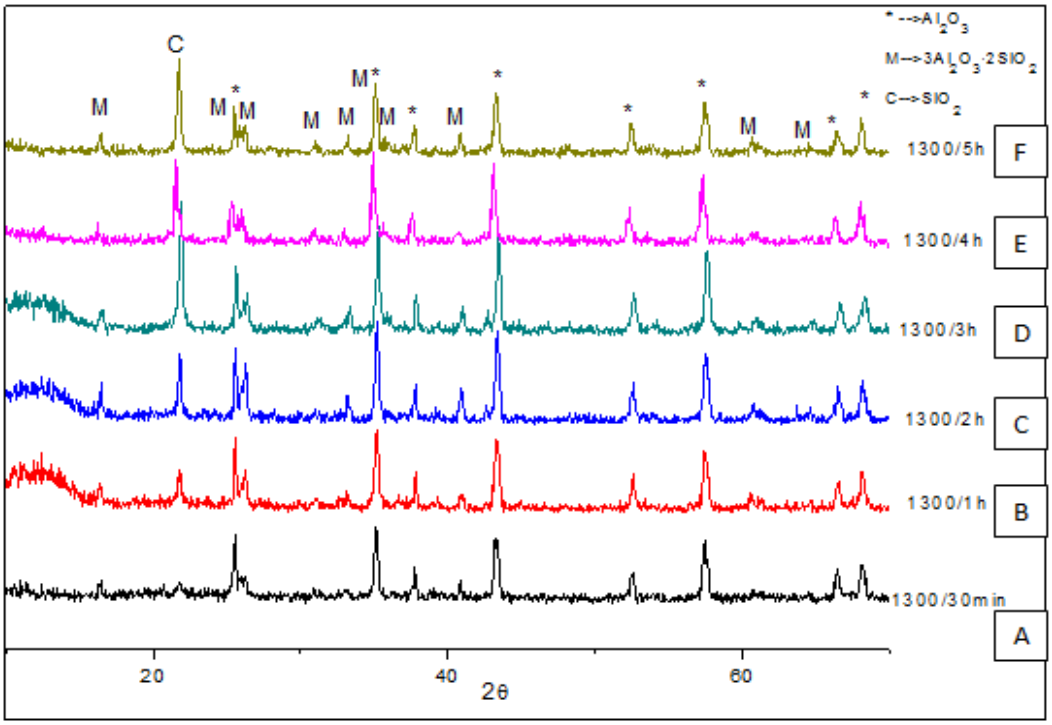

Figure 13. XRD patterns of the products after heat-treatment at 1300ºC for (a)30 min, (b)1 hour, (c)2 hours, (d)3 hours, (e) 4 hours and (f) 5 hours

SEM images of the mullite synthesis after heat treatment at 1000,1100, 1200 and 1300°C are shown in figure 14. The SEM images don't revealed a microstructure with characteristic mullite crystals when the temperature will increase. Figure 15 shows the SEM images of the mullite synthesis after heat treatment at 1300°C for 30 minutes to 300 minutes. The analysis does not show with certainty what is the crystalline structure of the mullite phase nor the other phases that are present as the cristobalite or corundum as we can see in the DRX.

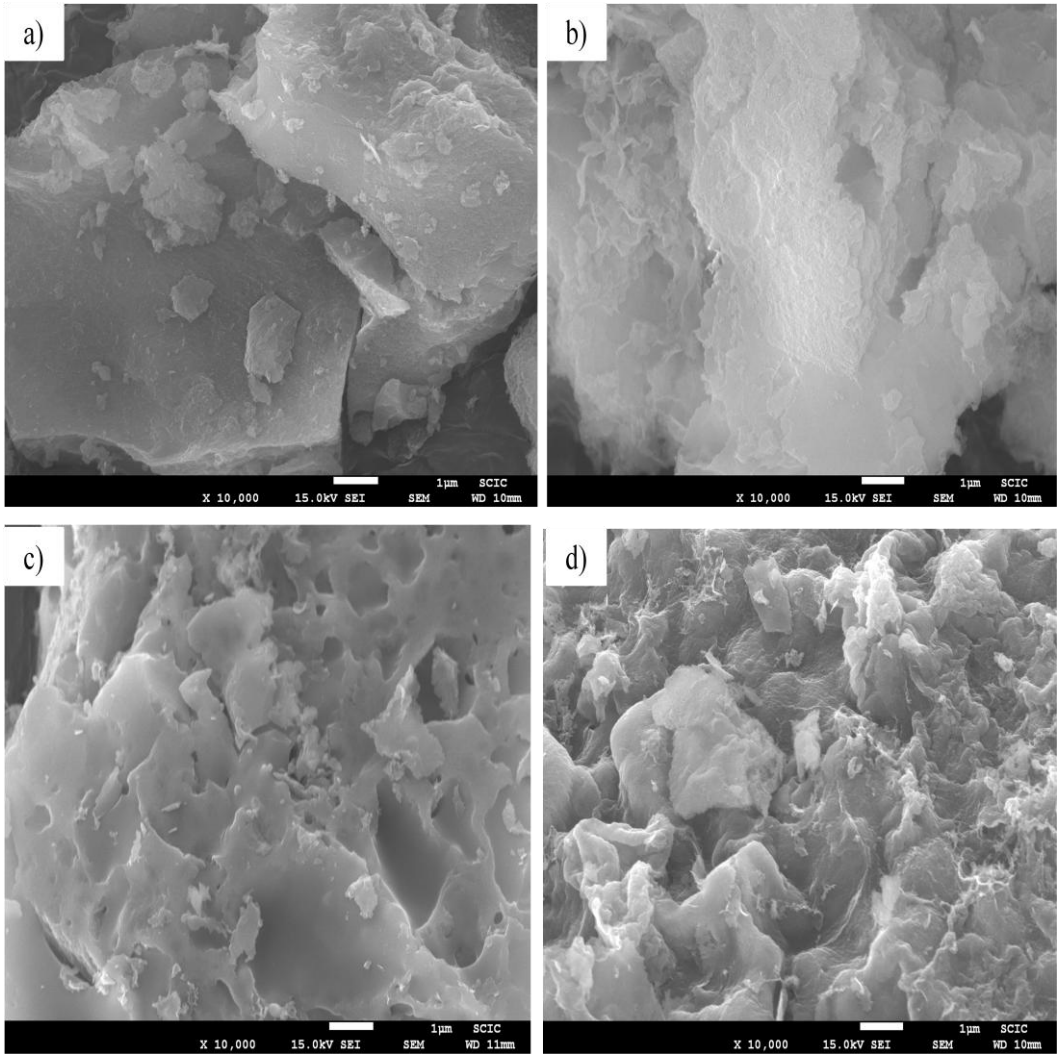

Figure 14. SEM images of samples heated at different temperatures a) 1000°C b) 1100°C c) 1200°C d)1300°C

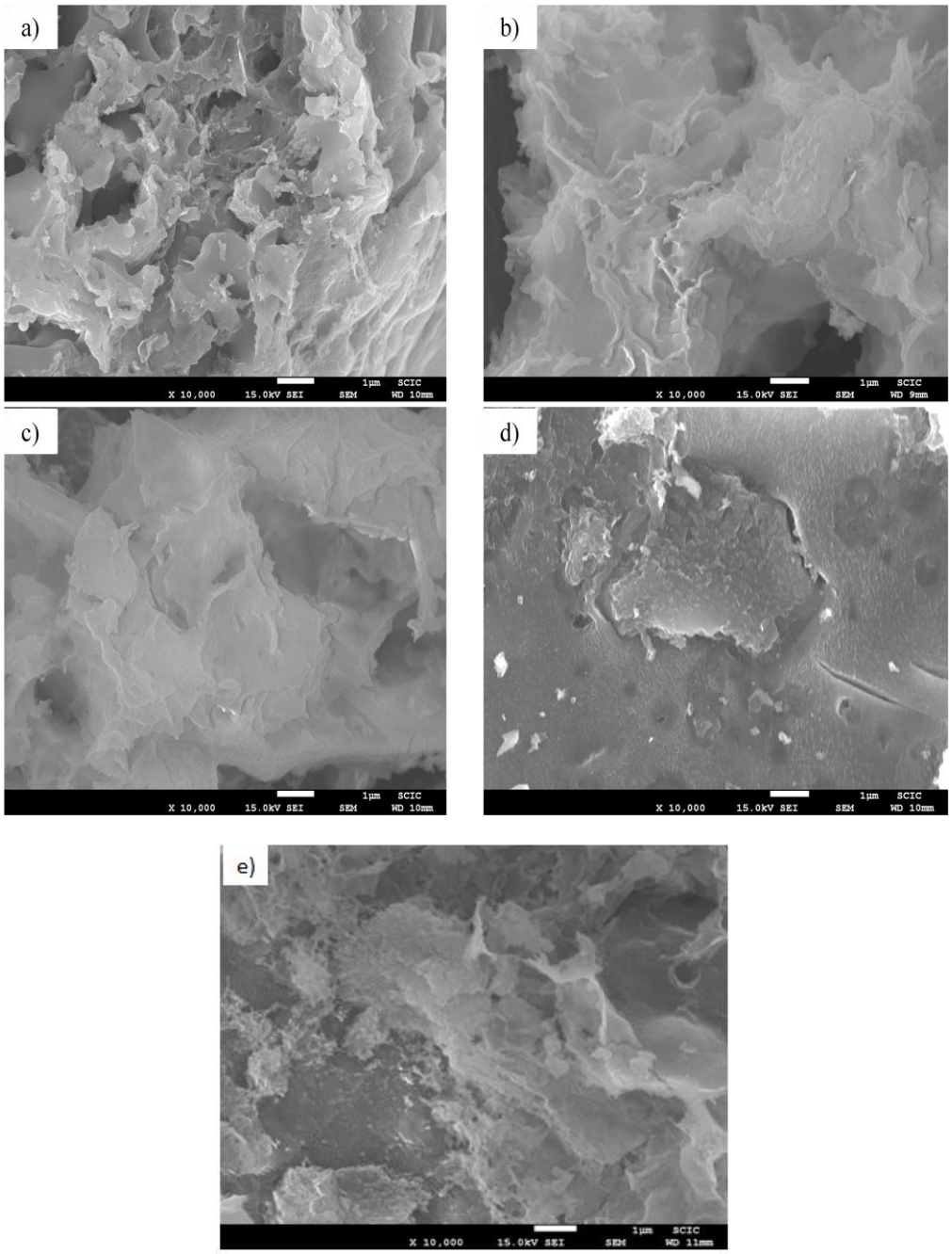

Figure 15. SEM images of samples heated at different times a) 1 hour b) 2 hour c)3 hours d)4hours e) 5hours

The results of EDX analysis are presented in tables 3 and 4. The total content of oxides that form the mullite are in the table. The global quantification gave the expected contents of Al_2O_3 and SiO_2 equivalent to the proposed stoichiometric relation. In particular, the thermal treatments at 1200-1300°C during 2-3 hours present the best results. Although a problem may be that it does not have the correct zone, the

mullite and therefore, these values can be diverted because the area that has reference to the crystalline phase of the mullite is not known.

Other studies have suggested that the good composition corresponding to the mullite phase is 70% of Al_2O_3 and 30% of SiO_2[5,46].

Table 3 . Results of EDX analysis.

Thermal treatment	Al_2O_3 (Compd %)	SiO_2 (Compd %)
1000ºC-30 minutes	69,34	18,78
1100ºC-30 minutes	58,53	41,47
1200ºC-30 minutes	63,52	36,48
1300ºC-30 minutes	71,88	28,12

Table 4. Results of EDX analysis.

Thermal treatment	Al_2O_3 (Compd %)	SiO_2 (Compd %)
1300ºC-1 hour	65,81	34,19
1300ºC-2 hours	67,46	32,54
1300ºC-3 hours	56,81	43,19
1300ºC-4 hours	71,57	28,43
1300ºC-5 hours	68,65	31,35

4.2 Functionalization of glass fibers

The effect of grinding on the glass fibers is shown in figure 16. Figure 16a shows that the fibers that are grinding by hand have the lengths between 50 and 100 μm. Figure 16 b shows that the fibers that are grinding by hand have the lengths between 10 and 50 μm. Figure 16 c and d shows a similar length between 1 and 25 μm, therefore, it is not necessary to continue analyzing the glass fibers after 20 seconds of grinding.

The different type of grinding gives us information on the length of the particles of the glass fibers to have a reference of how the size of these particles should be so that this process is reproducible in a safe way.

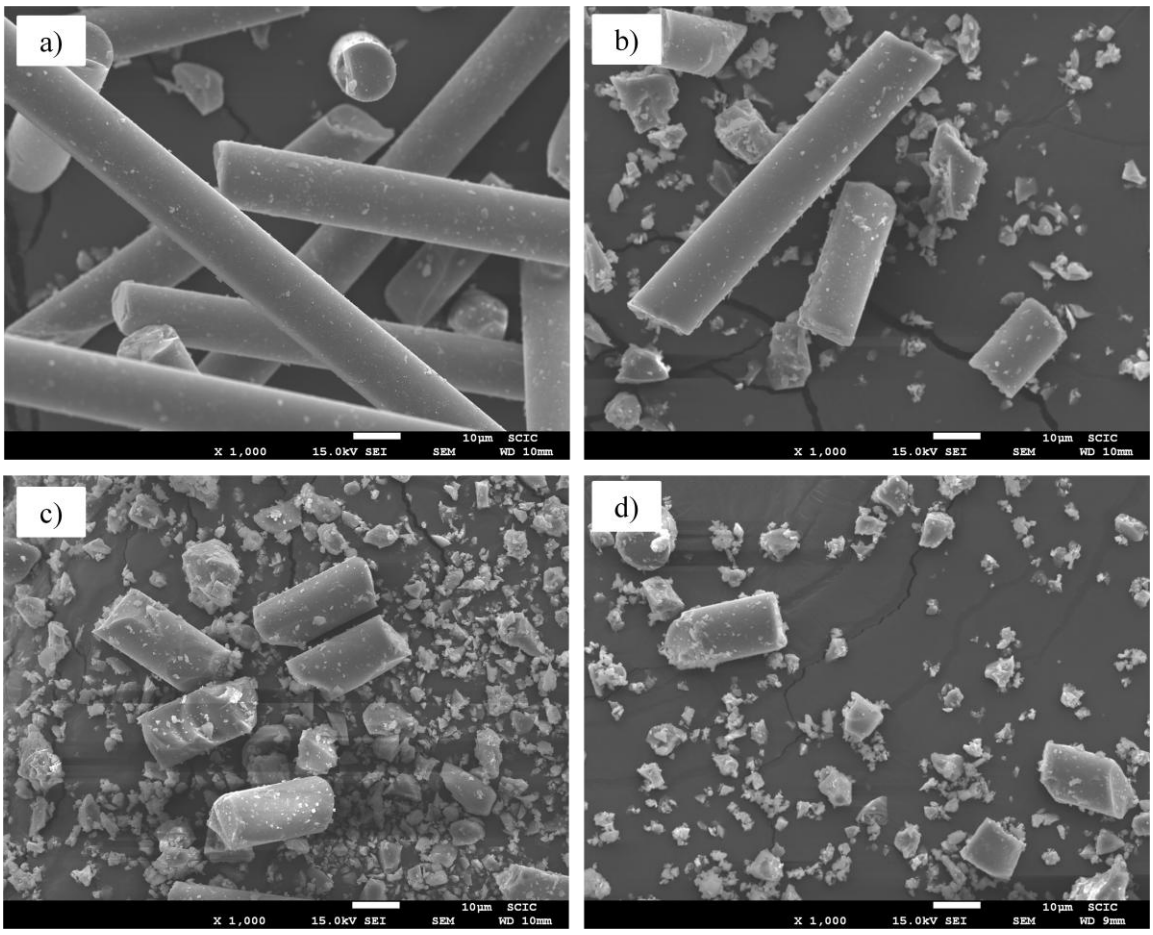

Figure 16. SEM images of glass fibers grinding by a)Hand b)ring mill 5'', c ring mill 10''and d) ring mill 20''.

Figure 17 shows the grinding glass fibers functionalized with mullite crystals. The fibers without heat treatment are in figure 17 a and c. These images show how a thicker and more compact structure is formed, although the heat treatment has not been carried out and, therefore, the crystalline phase of the mullite is not formed. The reason is because the porcelain stoneware treatment is carried out at 1200°C.

Figure 17 b and d presents fibers with heat treatment. The figure 23 b also shows a more compact structure, in this case the mullite phase is formed. On the other

hand, in figure 17 d, we observe that the structures are smaller than in the rest, although the mullite phase is also found

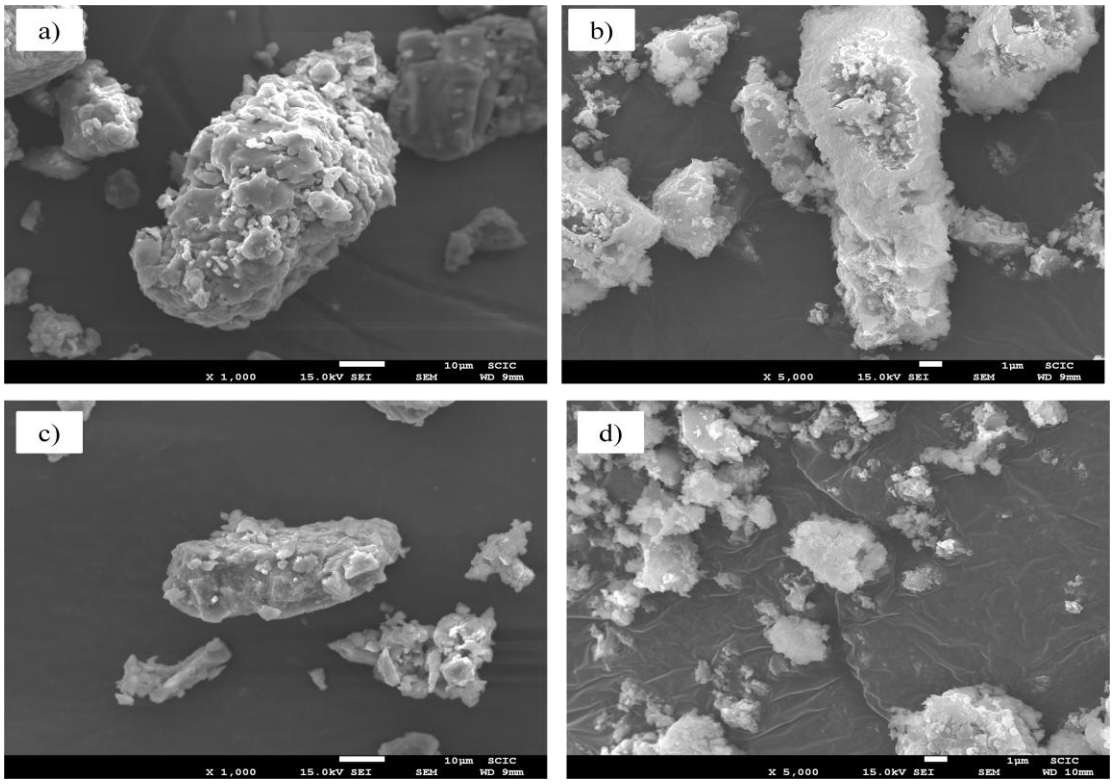

Figure 17. a) Functionalized glass fibers with mullite crystals and grinded at a) 5'' without thermal treatment, b) 5'' with thermal treatment c) 10'' without thermal treatment and d) 10'' with thermal treatment

Fiber particle size are observed in figure 18. It is observe how the % of volume glass fibers grinded by hand is between 10-100 microns. In contrast, the fibers grinded with the ring mill 5 seconds show more % volume in particles that have a size between 6-30 and fibers grinded with ring mill 5 and 10 seconds show less % volume but small size of particles.

Table 5 indicates the parameters of how the particles are distributed. It is observed that for the sample grinded by hand, only 40% of the particles are below 25 microns, while in the case of milling with ring mill it is observed that more than 85% of the particles are below of this value; being the samples milled at 10 and 20 seconds those that show a greater grinding. As the grinding at 10 and 20 seconds is very similar, it is decided not to continue with the grinding at 20 seconds.

The difference of grinding with ring mills at 5 seconds and at 10 is shown in that the percentage at 10 microns and at 1 micron is much higher at 10 seconds.

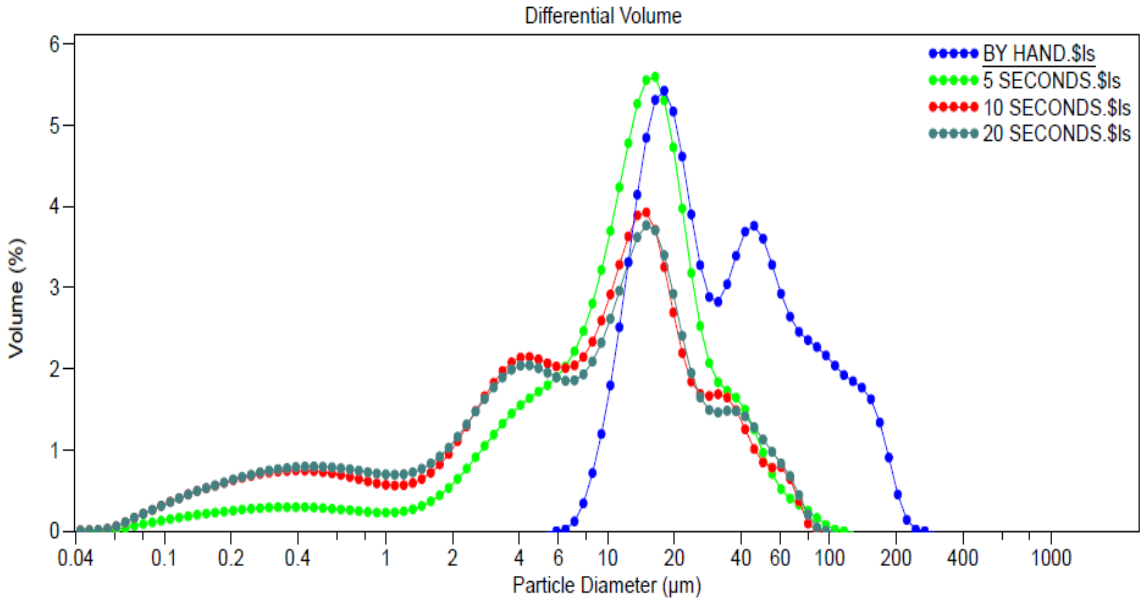

Figure 18 . Particle diameter in differents modes

Table 5 . Particle diameter in differents modes

	<100 µm	**<90 µm**	**<75 µm**	**<50 µm**	**<25 µm**	**<10 µm**	**<1 µm**
By hand	87.7%	85.2%	80.7%	67.9%	43.5%	2.73%	0%
5 Seconds	99.97%	99.9%	99.4%	97.0%	84.1%	38.4%	6.58%
10 Seconds	100%	100%	99.8%	96.8%	86.1%	55.3%	16.6%
20 Seconds	100%	99.98%	99.7%	96.2%	85.5%	55.3%	17.6%

Figure 19 shows the pieces calcined at the temperature of the porcelain stoneware that contain glass fibers that have been ground by hand .The pieces that refer to figure 19 a and c show points referring to glass fibers because hand grinding is not the most appropriate technique.

The figure 20 shows mix pieces with and without thermal treatment but in this but in this case, glass fibers were grinding by the ring mill at 5 and 10 seconds. The pieces without thermal treatment have a more brown tone while those with the mullite phase have a more gray tone. The difference in the type of grinding means that points referring to glass fibers are not detected.

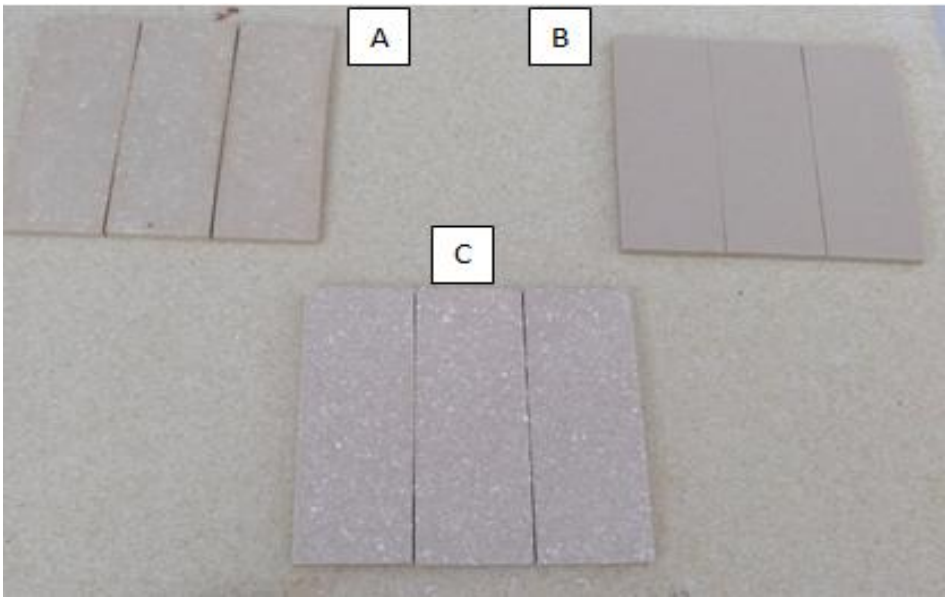

Figure 19. Pieces calcined with A) Fiberglass without calcined, B) Alone.and C) Mullite

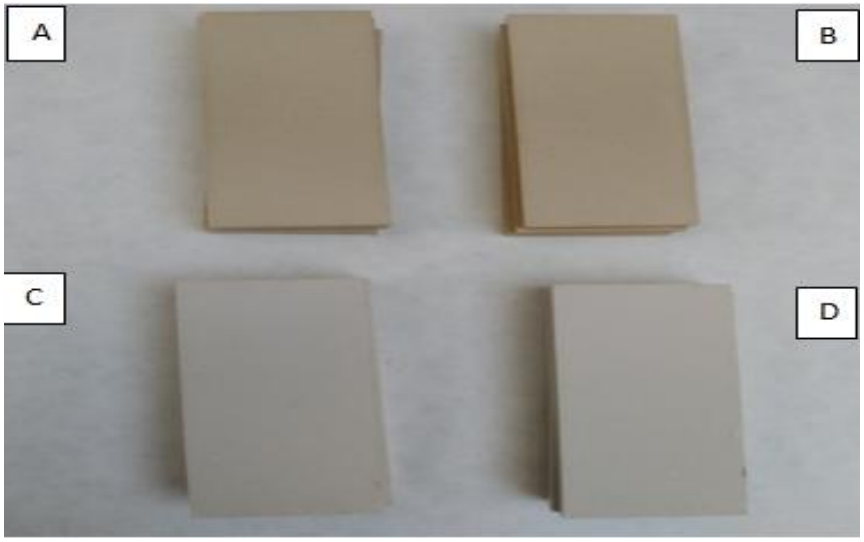

Figure 20. Pieces with grinding glass fibers with ring mill A) Without thermal treatment and 5'',B) Without thermal treatment and 10'' ,C) With thermal treatment and 5'' and D) With thermal treatment and 10''

The results of the flexural strength of the different compositions studied are shown in tables 6 and 7, where it can be concluded that although the addition of recycled glass causes an increase in mechanical resistance in the different materials, this has not occurred.

Table 6 shows the comparison of flexible strength of the reference pieces with the pieces milled by hand with treatment and without heat treatment. It is observed

how the mechanical resistance with glass fibers is lower than the reference pieces. The striking case is that the pieces that have been made with thermal treatment have less mechanical resistance than those that do not have the mullite phase formed.

Table 7 shows the comparison of flexible strength of the pieces milled with the ring mill at 5 and 10 seconds with treatment and without heat treatment. In this case, the calcined pieces that contain the mullite phase have greater mechanical resistance than the pieces without thermal treatment, which is more normal for the objective sought.

Table 6. Densities and mechanical strength in fibers crushed by hand.

Name	Dry density (g/cm^3)	Calcined density(g/cm^3)	Mechanical strength (Kg/cm^2)
Reference	1,94	2,38	469,3
Raw glass fibers 1	2,00	2,23	448,1
Raw glass fibers 2	1,99	2,21	397
Raw glass fibers 3	2,00	2,24	421,5
Calcined glass fibers 1	1,97	2,27	391,5
Calcined glass fibers 2	1,95	2,26	330,1
Calcined glass fibers 3	1,98	2,27	347,4

Table 7. Densities and mechanical strength in fibers crushed by ring mill 5 and 10 seconds.

Name	Dry density (g/cm^3)	Calcined density(g/cm^3)	Mechanical strength (Kg/cm^2)
Raw glass fibers 1 (5´)	1,90	2,26	347,84
Raw glass fibers 2 (5´)	1,92	2,26	374,37
Raw glass fibers 3 (5´)	1,93	2,26	423,71
Calcined glass fibers 1 (5´)	1,90	2,33	393,39
Calcined glass fibers 2 (5´)	1,92	2,32	551,43
Calcined glass fibers 3 (5´)	1,91	2,32	524,22
Raw glass fibers 1 (10´)	1,92	2,27	362,86
Raw glass fibers 2 (10´)	1,93	2,27	317,98
Raw glass fibers 3 (10´)	1,92	2,28	310,86
Calcined glass fibers 1 (10´)	1,92	2,30	415,34
Calcined glass fibers 2 (10´)	1,92	2,35	421,89
Calcined glass fibers 3 (10´)	1,91	2,33	402,59

5. Conclusion

The results obtained in XRD show us that the optimal thermal treatment for the formation of mullite is at 1300°C during 2 hours. From these conditions, the different tests have been carried out to obtain the porcelain stoneware tiles.
In the SEM technique, no differences were observed in the different treatments. When analyzing the glass fibers that have been ground by hand or crushed with the ring mill, it is observed how the particles have a very large size when made by hand while as we increase the grinding time, the size decreases.

Different concentrations of the oxides that refer to mullite are observed. The optimum temperature would be around 1200-1300ºC since it has a composition close to 70% of Al_2O_3 and 30% of SiO_2. As for the treatment time, the best option would be around 2-3 hours. As the porcelain stoneware treatment is carried out at 1200 ° C, the procedure without calcining has also been carried out to compare the results.

Regarding the main aim of the project, grinding the glass fibers with the ring mill for 5 seconds and its subsequent functionalization, the mechanical resistance of the porcelain tiles has been improved by 17%. Knowing the particle size allows the method to be reproducible.

6. REFERENCES

[1] A. L. Cavalieri, P. Pena, and S. De Aza, “Mullita: Naturaleza de la fusión y rango de solución sólida,” vol. 29, no. 3, pp. 171–176, 1990.

[2] A. K. CHAKRAVORTY and D. K. GHOSH, “Synthesis and 980oC Phase Development of Some Mullite Gels,” *J. Am. Ceram. Soc.*, vol. 71, no. 11, pp. 978–987, 1988.

[3] J. A. Pask and A. P. Tomsia, “Formation of Mullite from Sol-Gel Mixtures and Kaolinite,” *J. Am. Ceram. Soc.*, vol. 74, no. 10, pp. 2367–2373, 1991.

[4] T. Ebadzadeh, “Formation of mullite from precursor powders: sintering, microstructure and mechanical properties,” *Mater. Sci. Eng. A*, vol. 355, no. 1–2, pp. 56–61, 2003.

[5] P. J. Sánchez-Soto, D. Eliche-Quesada, S. Martínez-Martínez, E. Garzón-Garzón, L. Pérez-Villarejo, and J. M. Rincón, “The effect of vitreous phase on mullite and mullite-based ceramic composites from kaolin wastes as by-products of mining, sericite clays and kaolinite,” *Mater. Lett.*, vol. 223, pp. 154–158, 2018.

[6] H. Schneider, J. Schreuer, and B. Hildmann, “Structure and properties of mullite—A review,” *J. Eur. Ceram. Soc.*, vol. 28, no. 2, pp. 329–344, 2008.

[7] I. A. Aksay, D. M. Dabbs, and M. Sarikaya, “Mullite for Structural, Electronic, and Optical Applications,” *J. Am. Ceram. Soc.*, vol. 74, no. 10, pp. 2343–2358, 1991.

[8] Conference Committee, “The Final Proceedings for Mullite and Mullite Ceramics.” International Workshop, Irsee-Germany, 1994

[9] G. Mata-Osoro, J. S. Moya, M. Morales, L. A. Díaz, H. Schneider, and C. Pecharromán, “Faradaic current in different mullite materials: single crystal, ceramic and cermets.”

[10] A. Schrijnemakers *et al.*, “Mullite coatings on ceramic substrates: Stabilisation of Al_2O_3–SiO_2 suspensions for spray drying of composite granules suitable for reactive plasma spraying,” *J. Eur. Ceram. Soc.*, vol. 29, no. 11, pp. 2169–2175, 2009.

[11] G. Di Girolamo, C. Blasi, L. Pilloni, and M. Schioppa, “Microstructural and thermal properties of plasma sprayed mullite coatings,” *Ceram. Int.*, vol. 36, no. 4, pp. 1389–1395, 2010.

[12] A. Schrijnemakers *et al.*, “Mullite coatings on ceramic substrates: Stabilisation of Al_2O_3–SiO_2 suspensions for spray drying of composite granules suitable for reactive plasma spraying,” *J. Eur. Ceram. Soc.*, vol. 29, no. 11, pp. 2169–2175, 2009.

[13] K. K. Chawla, Z. R. Xu, and J.-S. Ha, “Processing, structure, and properties of

mullite fiber/mullite matrix composites," *J. Eur. Ceram. Soc.*, vol. 16, no. 2, pp. 293–299, 1996.

[14] J. WU, F. R. JONES, and P. F. JAMES, "Continuous fibre reinforced mullite matrix composites by sol–gel processing: Part I Fabrication and microstructures," *J. Mater. Sci.*, vol. 32, no. 13, pp. 3361–3368, 1997.

[15] D. Belzanr and H. Q. S. Lnoeprrnn, "Crystal structure and compressibility of 3:2 mullite," *Am. Mineral.*, vol. 78, pp. 1192–196, 1993.

[16] Saalfeld, H. and Guse, W., "Structure refinement of 3:2-mullite ($3Al_2O_3 \cdot 2SiO_2$).," *N. Jb. Miner. Mh.*, no. H4, p. 145–150., 1981.

[17] R. J. Ancrr, R. K. Mcmullan, and C. T. Hpwrrr, "Substructure and superstructure of mullite by neutron diffraction," *Am. Mineral.*, vol. 76, pp. 332–342, 1991.

[18] R. Sadanaga, M. Tokonami, and Y. Takéuchi, "The structure of mullite, $2Al_2O_3 \cdot SiO_2$, and relationship with the structures of sillimanite and andalusite," *Acta Crystallogr.*, vol. 15, no. 1, pp. 65–68, 1962.

[19] H. Fischer, R. X. and Schneider, "The mullite-type family of crystal structures. In Mullite," *ed .H. Schneider S. Komar. Wiley-VCH, Weinheim*, p. 1–46., 2005.

[20] P. Fielitz, G. Borchardt, H. Schneider, M. Schmücker, M. Wiedenbeck, and D. Rhede, "Self-diffusion of oxygen in mullite," *J. Eur. Ceram. Soc.*, vol. 21, no. 14, pp. 2577–2582, 2001.

[21] D. J. Cassidy, J. L. Woolfrey, J. R. Bartlett, and B. Ben-Nissan, "The Effect of Precursor Chemistry on the Crystallisation and Densification of Sol-Gel Derived Mullite Gels and Powders," *J. Sol-Gel Sci. Technol.*, vol. 10, no. 1, pp. 19–30, 1997.

[22] N. L. Bowen and J. W. Grieg, "The System Al_2O_3–SiO_2," *J. Am. Ceram. Soc. 7*, pp. 238–54, 1924.

[23] E.C. Shears and W.A. Archibald, "Aluminosilicate refractories," *Iron Steel 27*, pp. 26–30–65, 1954.

[24] N.A. Toropov and F. Ya. Galakhov, “Solid solutions in the system Al_2O_3–SiO_2,” *Izv. Aka. Nauk SSSR Otd. Khim. Nauk*, 1958.

[25] S. ARAMAKI and R. ROY, “Revised Phase Diagram for the System Al_2O_3-SiO_2,” *J. Am. Ceram. Soc.*, vol. 45, no. 5, pp. 229–242, 1962.

[26] J. A. Pask and I.A. Aksay, “Stable and Metastable Equilibria in the System $Si0_2$-$A1_20_3$,” *J. Am. Ceram. Soc.58*, 1975.

[27] R. F. D. and J. A. Pask, “Diffusion and reaction studies in the system Al_2O_3–SiO_2,” *J. Am. Ceram. Soc. 55*, pp. 525–531, 1972.

[28] S. H. RISBUD and J. A. PASK, “Mullite Crystallization from SiO_2-Al_2O_3 Melts,” *J. Am. Ceram. Soc.*, vol. 61, no. 1–2, pp. 63–67, 1978.

[29] C.G. Bergeron and S.H. Risbud, “Introduction to Phase Equilibria in ceramics,” *Am. Ceram. Soc., Columbus, OH*, 1984.

[30] F. J. KLUG, S. PROCHAZKA, and R. H. DOREMUS, “Alumina-Silica Phase Diagram in the Mollite Region,” *J. Am. Ceram. Soc.*, vol. 70, no. 10, pp. 750–759, 1987.

[31] J.A. Pask, “The Al_2O_3–SiO_2 system: logical analysis of phenomenological experimental data, in Ceramic Microstructures: Control at the Atomic Level,” *A.P. Tomsia A.M. Glaeser (eds.), Plenum, New York, NY*, p. 255–262., 1998.

[32] I. C. R. Ester Barrachina Albert, D. F. and Chiva, and J. B. C. Castelló, “RECYCLING AND REUSE OF MATERIALS,” pp. 1–345, 2015.

[33] P. S. Jain, A., Aravindan, V., Jayaraman, S., Kumar, S. and S. Balasubramanian, R., Ramakrishna, S., Madhavi, and M. P., “Activated carbons derived from coconut shells as high energy density cathode material for Li-ion capacitors,” *Sci. Rep. 3*, pp. 1–6, 2013.

[34] R. Taer, E., Mustika, W. S., Agustino, F., Hidayu, N. and Taslim, “The Flexible Carbon Activated Electrodes made from Coconut Shell Waste for Supercapacitor Application,” *Earth Environ. Sci. 58*, pp. 1–6, 2017.

[35] S. K. and A. S. Rudra, “Morphologically tailored activated carbon derived from

waste tires as high-performance anode for Li-ion battery," *J. Appl. Electrochem. 48*, pp. 1–13, 2018.

[36] G. Oliveux, L. O. Dandy, and G. A. Leeke, "Current status of recycling of fibre reinforced polymers: Review of technologies, reuse and resulting properties," *Prog. Mater. Sci.*, vol. 72, pp. 61–99, 2015.

[37] S. J. Pickering, "Recycling technologies for thermoset composite materials—current status," *Compos. Part A Appl. Sci. Manuf.*, vol. 37, no. 8, pp. 1206–1215, 2006.

[38] J. Palmer, O. R. Ghita, L. Savage, and K. E. Evans, "Successful closed-loop recycling of thermoset composites," *Compos. Part A Appl. Sci. Manuf.*, vol. 40, no. 4, pp. 490–498, 2009.

[39] S. Y. Oliveira Nunes A, Barna R, "Recycling of carbon fiber reinforced thermoplastic resin waste by steamthermolysis: thermo-gravimetric analysis and bench-scale studies," *Proc. 4th Int. carbon Compos. Conf. (4th IC3)Arcachon, Fr.*, 2014.

[40] A. M. Cunliffe and P. T. Williams, "Characterisation of products from the recycling of glass fibre reinforced polyester waste by pyrolysis," *Fuel*, vol. 82, no. 18, pp. 2223–2230, 2003.

[41] S. J. Pickering, R. M. Kelly, J. R. Kennerley, C. D. Rudd, and N. J. Fenwick, "A fluidised-bed process for the recovery of glass fibres from scrap thermoset composites," *Compos. Sci. Technol.*, vol. 60, no. 4, pp. 509–523, 2000.

[42] E. Lester, S. Kingman, K. H. Wong, C. Rudd, S. Pickering, and N. Hilal, "Microwave heating as a means for carbon fibre recovery from polymer composites: a technical feasibility study," *Mater. Res. Bull.*, vol. 39, no. 10, pp. 1549–1556, 2004.

[43] K. H. Yoon, A. T. DiBenedetto, and S. J. Huang, "Recycling of unsaturated polyester resin using propylene glycol," *Polymer (Guildf).*, vol. 38, no. 9, pp. 2281–2285, 1997.

[44] K. Yoshida, H. Hyuga, N. Kondo, and H. Kita, “Synthesis of precursor for fibrous mullite powder by alkoxide hydrolysis method,” in *Materials Science and Engineering B: Solid-State Materials for Advanced Technology*, vol. 173, no. 1–3, pp. 66–71, 2010.

[45] J. Roy and S. Maitra, “Synthesis and characterization of sol-gel-derived chemical mullite,” *J. Ceram. Sci. Technol.*, vol. 5, no. 1, pp. 57–62, 2014.

[46] M. F. Serra, M. S. Conconi, M. R. Gauna, G. Suárez, E. F. Aglietti, and N. M. Rendtorff, “Mullite ($3Al_2O_3{\cdot}2SiO_2$) ceramics obtained by reaction sintering of rice husk ash and alumina, phase evolution, sintering and microstructure,” *J. Asian Ceram. Soc.*, vol. 4, no. 1, pp. 61–67, 2016.